

Systematic input scheme for many-boson Hamiltonians via quantum walk

Weijie Du^{1,*} and James P. Vary¹

¹*Department of Physics and Astronomy, Iowa State University, Ames, Iowa 50010, USA*

(Dated: July 19, 2024)

We develop a novel, systematic input scheme for many-boson Hamiltonians in order to solve field theory problems within the light-front Hamiltonian formalism via quantum computing. We present our discussion of this input scheme based on the light-front Hamiltonian of the two-dimensional ϕ^4 theory. In our input scheme, we employ a set of quantum registers, where each register encodes the occupation of a distinct boson mode as binaries. We squeeze the boson operators of each mode and present the Hamiltonian in terms of unique combinations of the squeezed boson operators. We design the circuit modules for these unique combinations. Based on these circuit modules, we block encode the many-boson Hamiltonian utilizing the idea of quantum walk. We demonstrate our input scheme by solving the low-lying spectra of the Hamiltonian utilizing the IBM Qiskit quantum simulator. We can incorporate the input scheme in this work with the input scheme for many-fermion Hamiltonians; they jointly offer new pathways to solving the structure and dynamics of field theory problems on future fault-tolerant quantum computers.

I. INTRODUCTION

Quantum field theory (QFT) reconciles quantum mechanics and special relativity and it has important applications in many fundamental areas of physics [1]. Nonperturbative, *ab initio* structure and dynamics solutions of QFT are challenging on classical computers due to the nature of quantum many-body problems [2]. Quantum computing hardwares and algorithms hold the promise to address such numerical challenges [3].

Although, it is not currently possible to solve realistic problems on quantum computers in a way that outcompetes the best classical computers, it is an important and challenging task to develop new quantum algorithms that are suitable for solving QFT problems via *ab initio* methods on future fault-tolerant quantum computers. Following pioneering work by Jordan, Lee and Preskill [4], many quantum algorithms have been proposed for treating the QFT problems via the lattice-based Hamiltonian formalism [5–20]. In this cutting-edge area, major research focuses on reducing the error of digitization and latticing the continuous field onto qubit degrees of freedom as well as reducing the scaling of the computational resources [6, 8].

Fewer works employ the alternative promising light-front (LF) Hamiltonian formalism [21, 22] in formulating the QFT problems in quantum computing. The LF Hamiltonian formalism has the attractive feature that the LF vacuum has a simple structure as the Fock vacuum is an exact eigenstate of the full normal-ordered LF Hamiltonian; this enables the systematic Fock-space expansion of the physical states [23]. To date, the LF Hamiltonian formalism has witnessed successful initial applications in describing relativistic bound-state problems and dynamics in quantum electrodynamics, quantum chromodynamics, and chiral field theories on classical computers [24–40]. Many quantum algorithms have also been proposed to solve the structure and dynamics of hadronic systems [41–48].

However, a systematic Hamiltonian input scheme is a missing corner stone for a general-purpose quantum algorithm in computing the bound-state and scattering properties of the QFT problems based on the LF Hamiltonian formalism. An efficient input scheme is critical for large-scale calculations on future quantum computers, where the construction of the many-body Hamiltonian matrix is highly nontrivial. In Refs. [49, 50], we proposed a systematic input scheme for second-quantized many-fermion Hamiltonians. This input scheme respects the symmetries of the many-fermion Hamiltonians and is flexible for incorporating the particle-number variations. Yet, it is still an important mission to develop the counterpart Hamiltonian input scheme for many-boson systems. One noticeable difficulty that hinders such a development comes from the Bose-Einstein statistics, where multiple bosons can occupy the same mode and such many-boson states require proper normalization [51]. This is in contrast to the many-fermion case where the Pauli exclusion principle holds and the many-fermion states do not encounter multiple-occupancy normalization factors.

In this work, we introduce a novel and systematic input scheme for the many-boson Hamiltonians in quantum computing. We work in the second-quantized representation. Compared to the prototype sparse-matrix-based Hamiltonian input models [52, 53] that work with the row and column indices of the Hamiltonian matrices in the framework of first quantization, our input model operates directly on the Fock states and offers a convenient approach to access

* Email: duweigy@gmail.com

the many-boson Hamiltonian matrix elements based on the Fock bases. Compared to the Hamiltonian input scheme based on the approach of linear combination of unitaries [54, 55], our input scheme avoids the nontrivial ‘‘Prepare Oracle’’ for extracting the Hamiltonian matrix elements, which can be demanding in gate cost.¹ Our input scheme respects the symmetries of the many-boson Hamiltonians by design. It also enables a straightforward approach to prepare the many-boson states with desired symmetries on quantum computers. We provide an explicit and systematic circuit design for our input model in this work. This is to be compared with alternative input scheme of many-boson Hamiltonians [56] that is based on abstract controlled arithmetic operations that might be complicated to achieve on quantum computers.

We present the discussion of our input scheme utilizing the two-dimensional ϕ^4 $[(\phi^4)_2]$ theory as it is one of the simplest interacting QFT problems, and illustrates the essential ideas and techniques. We address the difficulty in normalizing the many-boson state by introducing the squeezed (or scaled) boson operators. We also present explicit circuit designs of the squeezed boson operators as well as their combinations, which properly treats the normalization of many-boson states and encodes the normalization as the phases of qubit states. Based on these techniques, we show the construction of the quantum walk states [52, 53, 57] to block encode the many-boson Hamiltonian. Utilizing this input scheme, we can quantum compute the structure and dynamics of the many-boson system utilizing precise and efficient quantum algorithms [58–61]. We demonstrate our input model by solving the spectrum of the LF Hamiltonian of the $(\phi^4)_2$ theory, where such spectral solutions shed lights on the phase transition of the $(\phi^4)_2$ theory [62, 63].

The arrangement of this paper is as follows. We present the $(\phi^4)_2$ theory within the LF Hamiltonian formalism and discuss the basis choice in Sec. II. In Sec. III, we present the details of the Hamiltonian input scheme of the LF Hamiltonian of the $(\phi^4)_2$ theory. In Sec. IV, we demonstrate the input scheme via a numerical example, where we compute the eigenenergies based on our input scheme utilizing a quantum-classical algorithm. We summarize in Sec. V, where we also present an outlook. We provide additional details in the Appendix.

II. THEORY

A. LF Hamiltonian of the $(\phi^4)_2$ theory

In brief, we present necessary details of the LF Hamiltonian formalism of the $(\phi^4)_2$ theory. Interested readers are referred to Refs. [62, 63] for more details.

The Lagrangian density of the $(\phi^4)_2$ theory is

$$\mathcal{L} = \frac{1}{2}(\partial_\mu\phi\partial^\mu\phi - m^2\phi^2) - \frac{\lambda}{4!}\phi^4, \quad (1)$$

where m denotes the mass parameter while λ is the coupling constant. One chooses $\lambda > 0$ and $m > 0$ so that the corresponding LF Hamiltonian is bounded and the vacuum state is the normal vacuum for small coupling in the symmetric phase of the theory. Following the discrete light-cone quantization (DLCQ) approach [64–66], one obtains the total longitudinal momentum K and the LF Hamiltonian H . These are given by Eqs. (8-11) in Ref. [63] where the zero mode is neglected as

$$K = \sum_{k=1} k a_k^\dagger a_k, \quad (2)$$

$$H = H_{1\rightarrow 1} + H_{2\rightarrow 2} + H_{3\rightarrow 1} + H_{1\rightarrow 3}, \quad (3)$$

¹ We expect that the gate cost of the Prepare Oracle for inputting the matrix elements of a general Hamiltonian can be as demanding as that for preparing a high-dimensional state vector with arbitrary coefficients.

with

$$H_{1 \rightarrow 1} = \sum_k \frac{1}{k} \left[m^2 + \underbrace{\frac{\lambda}{4\pi} \frac{1}{2} \sum_l \frac{1}{l}} \right] a_k^\dagger a_k, \quad (4)$$

$$H_{2 \rightarrow 2} = \frac{\lambda}{4\pi} \sum_{k \leq l} \sum_{m \leq n} \frac{1}{N_{kl}^2} \frac{1}{N_{mn}^2} \frac{1}{\sqrt{klmn}} \left[a_k^\dagger a_l^\dagger a_m a_n \right] \delta_{(m+n), (k+l)}, \quad (5)$$

$$H_{3 \rightarrow 1} = \frac{\lambda}{4\pi} \sum_k \sum_{l \leq m \leq n} \frac{1}{N_{lmn}^2} \frac{1}{\sqrt{klmn}} \left[a_k^\dagger a_l a_m a_n \right] \delta_{k, (m+n+l)}, \quad (6)$$

$$H_{1 \rightarrow 3} = \frac{\lambda}{4\pi} \sum_k \sum_{l \leq m \leq n} \frac{1}{N_{lmn}^2} \frac{1}{\sqrt{klmn}} \left[a_n^\dagger a_m^\dagger a_l^\dagger a_k \right] \delta_{k, (m+n+l)}, \quad (7)$$

with $N_{kl} = 1$ for $k \neq l$ and $N_{kl} = \sqrt{2!}$ for $k = l$, and

$$N_{lmn} = \begin{cases} 1, & \text{for } l \neq m \neq n, \\ \sqrt{3!}, & \text{for } l = m = n, \\ \sqrt{2!}, & \text{for any two of } l, m, \text{ and } n \text{ are equal.} \end{cases} \quad (8)$$

The summations of k , l , m , and n run over positive integers for symmetric boundary conditions which is the choice adopted here. Here, $H_{1 \rightarrow 1}$ and $H_{2 \rightarrow 2}$ are Hermitian and $H_{3 \rightarrow 1}^\dagger = H_{1 \rightarrow 3}$. One notes that H preserve the evenness and oddness of the particle number of the many-boson system. The total longitudinal momentum K is a conserved quantity in the LF Hamiltonian formalism as indicated by the Kronecker deltas in the above expressions and $[H, K] = 0$. According to H , one can compute the eigenvalues of the $(\phi^4)_2$ theory. These eigenvalues are related to the mass spectrum of the invariant-mass operator

$$\hat{M}^2 = KH. \quad (9)$$

One can typically scale H with m^2 and rewrite the interaction theory as a function of a single dimensionless variable λ/m^2 for convenience [63]. With this scaling, H has the dimension of $[\text{MeV}]^2$ and K is dimensionless.

We define a_k^\dagger and a_k as the creation and annihilation operators for the mode with the longitudinal momentum k , respectively. These boson operators satisfy the commutation relations [51]

$$[a_m, a_n] = [a_m^\dagger, a_n^\dagger] = 0, \quad [a_m, a_n^\dagger] = \delta_{m,n}. \quad (10)$$

For the LF Hamiltonian H [Eq. (3)] retained in this work, we note that there are at most four boson operators in all the monomials.

We denote $|k^{r_k}\rangle$ to be the normalized many-boson state with r_k bosons being in the mode k . The actions of the boson operators on $|k^{r_k}\rangle$ are [51]

$$a_k^\dagger |k^{r_k}\rangle = \sqrt{r_k + 1} |k^{r_k+1}\rangle, \quad a_k |k^{r_k}\rangle = \sqrt{r_k} |k^{r_k-1}\rangle, \quad (11)$$

where we have $a_k |k^0\rangle = 0$ with $r_k = 0$ denoting zero occupation of the mode k . In this sense, we have the normalized state $|k^{r_k}\rangle$ as

$$|k^{r_k}\rangle = \frac{1}{\sqrt{r_k!}} (a_k^\dagger)^{r_k} |k^0\rangle. \quad (12)$$

We note that the underbraced term in Eq. (4) is logarithmically divergent [62, 67]. One can remove this logarithmic divergence by considering the normal-ordered Hamiltonian [68], which means that one ignores a divergent constant from the definition of the mass parameter in the Hamiltonian.

The $(\phi^4)_2$ theory has also been used for studying spontaneous symmetry breaking. However, spontaneous symmetry breaking arises at a critical coupling λ/m^2 whose value depends on the treatment of the zero mode [63, 69–71]. Evaluating the precise value for the critical coupling involves taking the continuum limit which is very challenging on classical computers due to the nature of the strong correlation in the quantum many-body problems. Quantum computing might be promising for addressing such challenges.

B. Basis choice and eigenvalue problem

Following the notation of Ref. [62], we denote a general Fock state as $|k^{r_k}, l^{r_l}, m^{r_m}, \dots\rangle$. The total longitudinal momentum of the Fock state is $kr_k + lr_l + mr_m + \dots$, which receives contributions from every single mode in the Fock state.

As K commutes with H , the LF Hamiltonian matrix elements between the Fock states with different K values vanish. Therefore, in practical DLCQ calculations, one can enumerate and retain the Fock bases with the fixed total longitudinal momentum [24, 33–36, 40]. Within the Fock bases set $\mathcal{B}_K \equiv \{|k^{r_k}, l^{r_l}, m^{r_m}, \dots\rangle\}$ of a specific K value, one evaluates the matrix of H , or equivalently, the matrix of \hat{M}^2 [Eq. (9)], and computes the mass spectrum of the $(\phi^4)_2$ theory. Based on the mass spectrum, one can interrogate the critical coupling constant for the vanishing mass gap of the many-boson system as a function of K , and extrapolate for the critical coupling in the limit of $K \rightarrow \infty$, i.e., the continuum limit [62, 63].

III. HAMILTONIAN INPUT SCHEME

In this section, we present the elements of our Hamiltonian input scheme. We begin with our strategy to squeeze the boson operators, and rewrite the many-boson Hamiltonian with the squeezed boson operators as well as their combinations. Then, we discuss the scheme to encode the many-boson states, and present the design of the circuit modules for the squeezed boson operators as well as their combinations. Based on these modules, we show our Hamiltonian input scheme utilizing the idea of quantum walk. Finally, we present the analysis of the qubit and gate cost of our input scheme.

A. Modified Hamiltonian

For the $(\phi^4)_2$ theory, we can rewrite Eq. (3) according to the unique types of monomials as

$$H = \underbrace{B_{j_0} a_k^\dagger a_k}_{H_{1 \rightarrow 1}} + \dots + \underbrace{B_{j_1} a_k^\dagger a_l^\dagger a_m a_n}_{H_{2 \rightarrow 2}} + \dots + \underbrace{B_{j_2} a_k^\dagger a_l a_m a_n}_{H_{3 \rightarrow 1}} + \dots + \underbrace{B_{j_3} a_n^\dagger a_m^\dagger a_l^\dagger a_k}_{H_{1 \rightarrow 3}} + \dots, \quad (13)$$

where we employ the subscripts $k, l, m, n \in [1, K]$ to specify the modes of the boson operators. B_{j_i} denotes the coefficient, with

$$B_{j_0} = \frac{1}{k}, \quad B_{j_1} = \frac{\lambda}{4\pi} \frac{1}{N_{kl}^2 N_{mn}^2} \frac{\delta_{m+n, k+l}}{\sqrt{klmn}}, \quad B_{j_2} = B_{j_3} = \frac{\lambda}{4\pi} \frac{1}{N_{lmn}^2} \frac{\delta_{m+n+l, k}}{\sqrt{klmn}}. \quad (14)$$

The dots denote the other monomials with the same types of operator structures as those shown explicitly.

In order to develop our input scheme for the many-boson Hamiltonian, we squeeze (or scale) the boson operators for the mode k according to the maximal occupation value $\Lambda_k = \lfloor K/k \rfloor$ that is consistent with the total longitudinal momentum K for the system as

$$b_k \equiv a_k / \sqrt{\Lambda_k}, \quad b_k^\dagger = a_k^\dagger / \sqrt{\Lambda_k}. \quad (15)$$

This leads to the following identities

$$b_k |k^{r_k}\rangle = \sqrt{\frac{r_k}{\Lambda_k}} |k^{r_k-1}\rangle, \quad \text{for } r_k \in [1, \Lambda_k], \quad (16)$$

$$b_k^\dagger |k^{r_k}\rangle = \sqrt{\frac{r_k+1}{\Lambda_k}} |k^{r_k+1}\rangle, \quad \text{for } r_k \in [0, \Lambda_k-1], \quad (17)$$

with $b_k |k^0\rangle = 0$. According to this scaling, we have the scaled normalization factor $\sqrt{r_k/\Lambda_k} \in (0, 1]$ for $r_k \in [1, \Lambda_k]$ in Eq. (16), and the factor $\sqrt{(r_k+1)/\Lambda_k} \in (0, 1]$ for $r_k \in [0, \Lambda_k-1]$ in Eq. (17). These scaled normalization factors, denoted as ξ_k , can be encoded in terms of the angles of the rotational gates [72] in the quantum circuit, as shown in the following text.

With the squeezed boson operators, we can rewrite H [Eq. (13)] as

$$H = \underbrace{B'_{j_0} b_k^\dagger b_k}_{H_{1 \rightarrow 1}} + \dots + \underbrace{B'_{j_1} b_k^\dagger b_l^\dagger b_m b_n}_{H_{2 \rightarrow 2}} + \dots + \underbrace{B'_{j_2} b_k^\dagger b_l b_m b_n}_{H_{3 \rightarrow 1}} + \dots + \underbrace{B'_{j_3} b_n^\dagger b_m^\dagger b_l^\dagger b_k}_{H_{1 \rightarrow 3}} + \dots, \quad (18)$$

with

$$B'_{j_0} = \frac{\Lambda_k}{k}, \quad (19)$$

$$B'_{j_1} = \frac{\lambda}{4\pi} \frac{1}{N_{kl}^2 N_{mn}^2} \sqrt{\frac{\Lambda_k \Lambda_l \Lambda_m \Lambda_n}{klmn}} \delta_{m+n, k+l}, \quad (20)$$

$$B'_{j_2} = B'_{j_3} = \frac{\lambda}{4\pi} \frac{1}{N_{lmn}^2} \sqrt{\frac{\Lambda_k \Lambda_l \Lambda_m \Lambda_n}{klmn}} \delta_{m+n+l, k}. \quad (21)$$

The boson modes k, l, m, n in H are not necessarily different. In this sense, we can group the squeezed boson operators according to the modes in each monomial, while preserving the ordering of the creation and annihilation operators in view of the commutation relations. For example, with $k \neq l \neq m$, we can rewrite $b_k^\dagger b_l^\dagger b_l b_k$ and $b_k^\dagger b_k^\dagger b_l b_m$ as $(b_k^\dagger b_k)(b_l^\dagger b_l)$ and $(b_k^\dagger b_k^\dagger)(b_l)(b_m)$, respectively. With this grouping for all the monomials in H , we find that there are eight unique combinations $\{W_k\}$ of the squeezed boson operators that act on one single mode. We list these unique combinations in Table I, where we also present other details of these combinations.

TABLE I. Eight unique combinations of the squeezed boson operators. The first column lists all the unique combinations W_k of the squeezed boson operators. The second column presents the notations $(\cdot)_k$ of the circuit modules for W_k . The third column presents the scaled normalization factors ξ_{r_k} of the many-boson state obtained from the action of W_k on $|k^{r_k}\rangle$ [Eq. (24)] for $r_k \in [r_{k,i}, r_{k,f}]$ (fourth column). The fifth column presents the r_k values that belong to the vanishing cases in the practical circuit design of $(\cdot)_k$. The rightmost column presents the increment and decrement Δ_k in the occupation r_k when W_k acts on $|k^{r_k}\rangle$.

W_k	$(\cdot)_k$	scaled normalization factors ξ_{r_k}	$[r_{k,i}, r_{k,f}]$	vanishing cases	Δ_k
b_k^\dagger	$(+)_k$	$\sqrt{(r_k+1)/\Lambda_k}$	$[0, \Lambda_k - 1]$	Λ_k	+1
$b_k^\dagger b_k^\dagger$	$(++)_k$	$\sqrt{(r_k+1)(r_k+2)/\Lambda_k^2}$	$[0, \Lambda_k - 2]$	$\Lambda_k - 1, \Lambda_k$	+2
$b_k^\dagger b_k^\dagger b_k^\dagger$	$(+++)_k$	$\sqrt{(r_k+1)(r_k+2)(r_k+3)/\Lambda_k^3}$	$[0, \Lambda_k - 3]$	$\Lambda_k - 2, \Lambda_k - 1, \Lambda_k$	+3
b_k	$(-)_k$	$\sqrt{r_k/\Lambda_k}$	$[1, \Lambda_k]$	0	-1
$b_k b_k$	$(--)_k$	$\sqrt{r_k(r_k-1)/\Lambda_k^2}$	$[2, \Lambda_k]$	0, 1	-2
$b_k b_k b_k$	$(---)_k$	$\sqrt{r_k(r_k-1)(r_k-2)/\Lambda_k^3}$	$[3, \Lambda_k]$	0, 1, 2	-3
$b_k^\dagger b_k$	$(+ -)_k$	r_k/Λ_k	$[1, \Lambda_k]$	0	0
$b_k^\dagger b_k^\dagger b_k b_k$	$(+ + - -)_k$	$r_k(r_k-1)/\Lambda_k^2$	$[2, \Lambda_k]$	0, 1	0

B. Basis encoding scheme

Recall that we retain the Fock basis set \mathcal{B}_K with fixed total longitudinal momentum K and omit the zero mode in this work. In order to encode the Fock states in \mathcal{B}_K , we choose to implement the quantum register s that consists of a set of subregisters $\{s_k\}$: for the mode $k \in [1, K]$, we apply the compact mapping to encode the occupation r_k as binaries in the subregister s_k . Following this scheme, as an example, we can encode the Fock state $|\mathcal{F}\rangle = |k^{r_k}, l^{r_l}, m^{r_m}\rangle$ with $1 \leq k < l < m \leq K$ as the register state

$$|0\rangle_{s_1} \cdots |r_k\rangle_{s_k} \cdots |r_l\rangle_{s_l} \cdots |r_m\rangle_{s_m} \cdots |0\rangle_{s_K}, \quad (22)$$

where the occupations r_k, r_l , and r_m are encoded in the binary representation. We adopt the notation $|\cdot\rangle_{reg}$ to specify the state of the quantum register “reg”. We occasionally omit the subscript when there is no risk of confusion.

C. Circuit representation of W_k

We discuss the design of the circuit module $(\cdot)_k$ for the combination W_k of the squeezed boson operators in this section. Indeed, this module can be understood as the “circuit representation” of W_k . A schematic circuit design of $(\cdot)_k$ is shown in Fig. 1(a).

We recall that the occupation r_k of the mode k is encoded as binaries in the subregister s_k . For each s_k , we employ a single qubit ph_k , which is initialized as $|0\rangle$. Jointly, the set of qubits $\{ph_k\}$ make up the register ph . Then, we

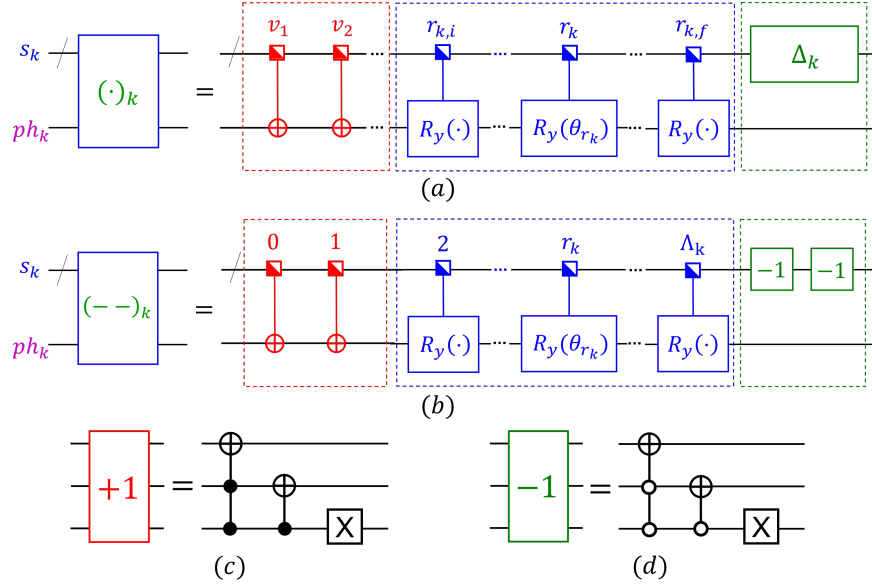


FIG. 1. (color online) Schematic design of the circuit module $(\cdot)_k$ of W_k in Table I. Panel (a) presents the general scheme of the circuit design of $(\cdot)_k$, where v_1, v_2, \dots denote the occupation numbers for the vanishing cases. Panel (b) shows an illustration of the circuit design of the module $(--)_k$ that corresponds to $W_k = b_k b_k$. Panels (c) and (d) are the examples of the circuit designs of the quantum adder “+1” and subtractor “-1” for one-unit increment and decrement in the three-qubit case, respectively. The slashed line denotes a register that may contain several qubits. The half-filled squares denote the controlling conditions for the quantum operations; these conditions can be constructed according to corresponding occupation values above the squares. The dot in each R_y gate denotes the corresponding rotational angle.

design the circuit module $(\cdot)_k$ to conduct the following operations on the register states

$$|r_k\rangle_{s_k} |0\rangle_{ph_k} \xrightarrow{(\cdot)_k} |r_k + \Delta_k\rangle_{s_k} |\gamma_{r_k}\rangle_{ph_k}, \quad (23)$$

where $|\gamma_{r_k}\rangle = |\xi_{r_k}\rangle = \xi_{r_k} |0\rangle + \sqrt{1 - \xi_{r_k}^2} |1\rangle$ for $r_k \in [r_{k,i}, r_{k,f}]$ (fourth column in Table I). Here, $\xi_{r_k} \in (0, 1]$ is the scaled normalization factor and Δ_k denotes the change in r_k . The values of ξ_{r_k} and Δ_k are shown in the third column and the rightmost column in Table I, respectively. In practical design of the circuit module $(\cdot)_k$, it is convenient to specify the “vanishing cases” (fifth column in Table I). These correspond to the cases where $W_k |k^{r_k}\rangle = 0$ or $W_k |k^{r_k}\rangle \propto |k^{r_k+\Delta_k}\rangle$ with $(r_k + \Delta_k) > \Lambda_k = \lfloor K/k \rfloor$. We set $|\gamma_{r_k}\rangle = |1\rangle$ for the r_k values that belong to such vanishing cases.

The circuit module $(\cdot)_k$ of the combination W_k can be achieved by the following analyses and constructions.

1. *Vanishing cases.* For each r_k value that belongs to the vanishing cases (fifth column in Table I), we flip the state of ph_k from $|0\rangle$ to $|1\rangle$ controlled by the subregister s_k being in the state $|r_k\rangle_{s_k}$.

2. *Nonvanishing cases.* For the nonvanishing cases with $r_k \in [r_{k,i}, r_{k,f}]$ (fourth column in Table I), we have

$$W_k |k^{r_k}\rangle = \xi_{r_k} |k^{r_k+\Delta_k}\rangle. \quad (24)$$

As for the corresponding circuit construction, we apply a set of $R_y(\theta_{r_k})$ gates [72] to the qubit ph_k , each of which is controlled by the state $|r_k\rangle_{s_k}$ with $r_k \in [r_{k,i}, r_{k,f}]$. We take the rotational angles as

$$\theta_{r_k} = 2 \arccos \xi_{r_k}, \quad (25)$$

such that the state of ph_k becomes $|\xi_{r_k}\rangle_{ph_k} \equiv R_y(\theta_{r_k}) |0\rangle_{ph_k}$. That is, ξ_{r_k} is encoded as the coefficient of the component $|0\rangle$ of the state $|\xi_{r_k}\rangle_{ph_k}$.

3. *Changes in the occupation.* To account for the change Δ_k in the occupation r_k recorded as the state $|r_k\rangle_{s_k}$, we can perform a sequence of quantum adders or subtractors [73] to the subregister s_k . These quantum arithmetic operators perform the following operation on the state of s_k :

$$|r_k\rangle_{s_k} \rightarrow |r_k + \Delta_k\rangle_{s_k}. \quad (26)$$

We illustrate the circuits of the quantum adder and subtractor in Figs. 1(c) and (d) for the three-qubit case, respectively.

The above completes the construction of the circuit module $(\cdot)_k$ corresponding to Eq. (23). As a specific example, we present in Fig. 1(b) the circuit module $(--)_k$ of $W_k = b_k b_k$.

D. Encoding many-boson Hamiltonian via quantum walk

We now present the input scheme of the LF Hamiltonian of the $(\phi^4)_2$ theory utilizing the idea of the quantum walk. We first construct the *forward* walk state. Provided the Fock state $|\mathcal{F}\rangle$, we start with the state of multiple quantum registers

$$|\Phi_0\rangle = |0\rangle_{id} |\mathcal{F}\rangle_s |0\rangle_{ph} |0\rangle_{me} |1\rangle_{ac}, \quad (27)$$

where the index register “*id*” is initialized as $|0\rangle$. The Fock state $|\mathcal{F}\rangle$ is encoded by the system register s that consists of a set of subregisters $\{s_k\}$ (with $k \in [1, K]$). The phase register “*ph*” contains K qubits $\{ph_k\}$. Each single-qubit subregister ph_k is initialized as $|0\rangle$ and is coupled with the subregister s_k . In addition, we adopt the single-qubit register “*me*” that is initialized as $|0\rangle$ to encode the coefficients $\{B'_j\}$ of the monomials of H [Eq. (18)]. Finally, we employ the single-qubit action register “*ac*” and initialize it as $|1\rangle$.

Based on $|\Phi_0\rangle$, we introduce the diffusion operator (which consists of a set of Hadamard gates) to the register *id* and obtain

$$|\Phi_1\rangle = \frac{1}{\sqrt{\mathcal{D}}} \sum_{j=0}^{\mathcal{D}-1} |j\rangle_{id} |\mathcal{F}\rangle_s |0\rangle_{ph} |0\rangle_{me} |1\rangle_{ac}. \quad (28)$$

We label each monomial in H [Eq. (18)] by a specific index $j \in [0, \mathcal{D} - 1]$. For the clarity of explanation, we take the j th monomial of H [Eq. (18)] to be $B'_j W_k W_l$ (with $1 \leq k < l \leq K$) as an example. Then, we implement the following operations controlled by $|j\rangle_{id}$.

Step 1. We apply the circuit module $(\cdot)_k$ of W_k to the subregisters s_k and ph_k , and the circuit module $(\cdot)_l$ of W_l to s_l and ph_l . According to Eq. (23), we have the operations on the state of registers s and ph as

$$|\mathcal{F}\rangle_s |0\rangle_{ph} \xrightarrow{(\cdot)_l(\cdot)_k} |\mathcal{F}_j\rangle_s |\Upsilon_j\rangle_{ph}. \quad (29)$$

Here, the Fock state $|\mathcal{F}\rangle$ is encoded as $|r_1\rangle_{s_1} \cdots |r_k\rangle_{s_k} \cdots |r_l\rangle_{s_l} \cdots |r_K\rangle_{s_K}$ in the register s . With the changes of the occupations in the modes k and l determined by W_k and W_l , we have the modified Fock state $|\mathcal{F}_j\rangle$ encoded as $|r_1\rangle_{s_1} \cdots |r_k + \Delta_k\rangle_{s_k} \cdots |r_l + \Delta_l\rangle_{s_l} \cdots |r_K\rangle_{s_K}$ in the register s . We also have the operation on the phase register ph as

$$\begin{aligned} |0\rangle_{ph} &= |0\rangle_{ph_1} \cdots |0\rangle_{ph_k} \cdots |0\rangle_{ph_l} \cdots |0\rangle_{ph_K} \\ \rightarrow |\Upsilon_j\rangle_{ph} &\equiv |0\rangle_{ph_1} \cdots |\gamma_{r_k}\rangle_{ph_k} \cdots |\gamma_{r_l}\rangle_{ph_l} \cdots |0\rangle_{ph_K}. \end{aligned} \quad (30)$$

Step 2. We operate on the single-qubit register me as

$$|0\rangle_{me} \rightarrow e^{i\beta_j} |\rho_j\rangle_{me}, \quad (31)$$

where $|\rho_j\rangle \equiv \rho_j |0\rangle + \sqrt{1 - \rho_j^2} |1\rangle$. The parameters β_j and ρ_j are determined from the identity

$$\rho_j e^{i\beta_j} = B'_j / \Xi, \quad (32)$$

with $\Xi \geq \max_j |B'_j|$ and $\rho_j = |B'_j / \Xi| \leq 1$. We take $\beta_j = 0$ as $B'_j > 0$ in the $(\phi^4)_2$ theory discussed in this work.² In other words, the coefficient B'_j , scaled by Ξ that is at least the max norm of all the coefficients $\{B'_j\}$ of H [Eq. (18)], is encoded by the register me as the coefficient of the component $|0\rangle$ of the state $e^{i\beta_j} |\rho_j\rangle_{me}$. Practically, the operation in Eq. (31) can be achieved by applying the phase gate $P_X(\beta_j)$ followed by a $R_y(\alpha_j)$ gate to the register me , where we take

$$P_X(\beta_j) |0\rangle = e^{i\beta_j} |0\rangle, \quad P_X(\beta_j) |1\rangle = |1\rangle, \quad \alpha_j = 2 \arccos \rho_j. \quad (33)$$

² In general applications, we take $\beta_j = \arg[B'_j / \Xi] \in (-\pi, \pi]$ as B'_j can be a complex number.

Step 3. We flip $|1\rangle_{ac}$ to $|0\rangle_{ac}$ by a Pauli X gate.

The above completes the operations on $|\Phi_1\rangle$, where these operations are based on the assumed form of the j th monomial $B_j^l W_k W_l$.

Analogously, we apply the same steps as described above for all the monomials in H [Eq. (18)], where each of these monomials is labeled by a distinct j . With these operations, we can construct the *forward* walk state

$$|\Phi_2\rangle = \frac{1}{\sqrt{\mathcal{D}}} \sum_{j=0}^{\mathcal{D}-1} |j\rangle_{id} |\mathcal{F}_j\rangle_s |\Upsilon_j\rangle_{ph} e^{i\beta_j} |\rho_j\rangle_{me} |b_j\rangle_{ac}, \quad (34)$$

where $b_j = 0$ if the index j indeed corresponds to a monomial in H ; b_j remains as 1 otherwise.³ In Fig. 2, we illustrate the circuit to construct the forward walk state via a simple example.

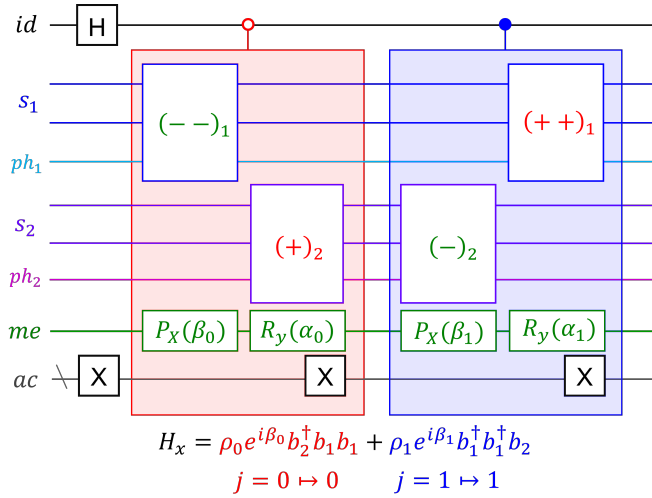


FIG. 2. (color online) Illustration of the circuit design of the forward walk state according to the Hamiltonian H_x of a simple many-boson system. The combinations of the squeezed boson operators and their circuit modules are shown in Table I and Fig. 1(a), respectively. The coefficient in the j th monomial (with $j = 0, 1$) is expressed as $\rho_j e^{i\beta_j}$ with $\rho_j \in (0, 1]$; it is encoded by a phase gate $P_X(\beta_j)$ with $P_X(\beta_j)|0\rangle = e^{i\beta_j}|0\rangle$ and $P_X(\beta_j)|1\rangle = |1\rangle$. The angle of the R_y gate [72] is $\alpha_j = 2 \arccos \rho_j$. For clarity, the subregisters s_k and ph_k with $k = 1, 2$ are coupled in the circuit.

Next, we construct the *backward* walk state based on the Fock state $|\mathcal{G}\rangle$ as

$$|\Psi_0\rangle = |0\rangle_{id} |\mathcal{G}\rangle_s |0\rangle_{ph} |0\rangle_{me} |0\rangle_{ac}, \quad (35)$$

where the register ac is initialized as $|0\rangle$ in this case. With the action of the diffusion operator on $|0\rangle_{id}$, we get

$$|\Psi_1\rangle = \frac{1}{\sqrt{\mathcal{D}}} \sum_{k=0}^{\mathcal{D}-1} |k\rangle_{id} |\mathcal{G}\rangle_s |0\rangle_{ph} |0\rangle_{me} |0\rangle_{ac}. \quad (36)$$

The walk states $|\Phi_2\rangle$ and $|\Psi_1\rangle$ block encode the many-boson Hamiltonian. In particular, the inner product of the walk states is

$$\langle \Psi_1 | \Phi_2 \rangle = \frac{1}{\mathcal{D}} \sum_{j=0}^{\mathcal{D}-1} \sum_{k=0}^{\mathcal{D}-1} e^{i\beta_j} \langle k | j \rangle_{id} \langle \mathcal{G} | \mathcal{F}_j \rangle_s \langle 0 | \Upsilon_j \rangle_{ph} \langle 0 | \rho_j \rangle_{me} \langle 0 | b_j \rangle_{ac}, \quad (37)$$

which correctly produces the many-boson matrix element of the scaled Hamiltonian $H' \equiv H/(\mathcal{D}\Xi)$ based on the Fock states $|\mathcal{F}\rangle$ and $|\mathcal{G}\rangle$. The kernel $\langle 0 | b_j \rangle_{ac} = \delta_{b_j, 0}$ removes the null contributions indexed by the j values that do not correspond to any monomial in the LF Hamiltonian.

³ Note that some of the j values encoded in the register id may not relate to any term in H in practical applications.

We can rewrite the walk states based on the isometries \mathcal{T}_1 and \mathcal{T}_2 as

$$|\Phi_2\rangle = \mathcal{T}_1 |\mathcal{F}\rangle_s \otimes |0\rangle_a, \quad |\Psi_1\rangle = \mathcal{T}_2 |\mathcal{G}\rangle_s \otimes |0\rangle_a, \quad (38)$$

where a denotes all the registers except the system register s . These walk states block encode the many-boson Hamiltonian as

$$\langle\langle \mathcal{G}|_s \otimes \langle 0|_a \mathcal{T}_2^\dagger \mathcal{T}_1 (|\mathcal{F}\rangle_s \otimes |0\rangle_a) = \frac{1}{\mathcal{D}\Xi} \langle \mathcal{G} | H | \mathcal{F} \rangle. \quad (39)$$

We comment that this Hamiltonian input scheme is non-Hermitian, i.e., $\mathcal{T}_2^\dagger \mathcal{T}_1 \neq (\mathcal{T}_2^\dagger \mathcal{T}_1)^\dagger$. Compared to the typical sparse-matrix input scheme discussed in Refs. [52, 53, 57] that access the Hamiltonian matrix elements according to their row and column indices, our input scheme dynamically computes the matrix element of the scaled many-boson Hamiltonian H' based on the Fock states [Eq. (37)]. Finally, we remark that our input scheme does not interact with any precomputed database. There is no need to uncompute any ancilla qubits, where such uncomputation procedures are necessary in the typical Hamiltonian input scheme [52, 53, 57].

E. Analysis of the gate and qubit cost

We estimate the gate cost of our Hamiltonian input scheme with the following analysis. We retain K modes in our calculations by setting the total longitudinal momentum to be K . In the most complicated case, there are $O(K^4)$ monomials in H [Eq. (18)].⁴ Expressed in terms of W_k , each monomial may contain four combinations of the squeezed boson operators (i.e., in the form of $W_k W_l W_m W_n$). It takes at most $\Theta(K)$ gates to construct the circuit module for each combination according to our design (Sec. III C). These are the dominant gate costs required to construct the forward walk state. In comparison, the gate cost to construct the backward walk state is much less than the gate cost required for constructing the forward walk state. Hence, the total gate cost to input the many-boson Hamiltonian scales as $\tilde{O}(K^5)$, where the tilde notation denotes that we suppress the logarithmic factor from compiling the multiple controlled gates [1, 74, 75]. We expect that this gate complexity can be significantly reduced in realistic implementations as (1) the number of monomials is much less than $O(K^4)$ due to the symmetries of the system (e.g., the momentum conservation); and (2) the maximal occupation $\Lambda_k = \lfloor K/k \rfloor$ of the mode k can be much less than K when k is large, which reduces the gate cost to construct the circuit module $(\cdot)_k$.

The qubit cost to input the Hamiltonian is dominated by the number of qubits necessary for the registers $s = \{s_k\}$ and $ph = \{ph_k\}$ for $k \in [1, K]$. According to our encoding scheme, we need $\log_2(\Lambda_k + 1)$ qubits to encode all the possible occupation values in the subregister s_k . As the maximal occupation of the mode k is $\Lambda_k = \lfloor K/k \rfloor$, the number of qubits required for the register s is

$$Q_s = \sum_{k=1}^K \lceil \log_2(\Lambda_k + 1) \rceil = \sum_{k=1}^K \lceil \log_2(\lfloor K/k \rfloor + 1) \rceil. \quad (40)$$

We note that Q_s grows approximately as $2K$ for large K . In addition, it takes K qubits for the register ph . In sum, the total number of qubits to block encode the many-boson Hamiltonian is approximately $\Theta(K)$, where we omit the minor qubit cost: (1) the two qubits required for the registers me and ac ; and (2) the $O(4 \log_2 K)$ qubits required for the register id to encode all the possible indices j of the monomials in H [Eq. (18)].

Kirby et al. [56] introduced a general-purpose Hamiltonian input scheme for many-particle systems, where the authors employ the compact basis encoding and the log-local operations for the controlled arithmetic calculations in order to reduce the cost of the quantum computing resources. As for the LF Hamiltonian of the $(\phi^4)_2$ theory discussed in this work, their input scheme [56] reports the gate complexity to be $O(K^3)$ and the qubit cost to be $O(K \log K)$. Our scaling of the quantum computing resources is close to theirs. However, it can be challenging to compile the abstract log-local operations employed in Ref. [56] to primitive gates in quantum computing. In comparison, our input scheme presents an explicit circuit based on straightforward applications of the elementary gates and their controlled versions. In this sense, it provides a realistic alternative to the input scheme in Ref. [56] for the many-boson Hamiltonian.

⁴ We adopt the conventional notations in computer science for the complexity analysis in this work. For the functions $w(x)$ and $v(x)$, $w(x) \in \Theta(v(x))$ denotes $\lim_{x \rightarrow \infty} \frac{w(x)}{v(x)} = c$ with c being some constant. The notation $w(x) \in O(v(x))$ means $\lim_{x \rightarrow \infty} \frac{w(x)}{v(x)} = 0$.

IV. NUMERICAL DEMONSTRATION AND DISCUSSIONS

We present the spectral calculations of the LF Hamiltonian of the $(\phi^4)_2$ theory based on our Hamiltonian input scheme in order to demonstrate its validity and utility. Though we restrict our discussions to the spectral calculations, we comment that our Hamiltonian input scheme can also be implemented with other efficient algorithms, such as the quantum signal processing [58], the quantum singular value transformation [59, 60], and the quantum eigenvalue transformation [61], etc., for dynamics simulations with optimal gate complexities with respect to the simulation error and time.

We adopt the algorithm of the Chebyshev-polynomial-based quantum Krylov subspace diagonalization (CP-QKSD) [76] for the eigenvalue calculations in our numerical example. The CP-QKSD algorithm makes use of the quantum computer to deal with the quantum many-body problems that can be intractable on classical computers, and cast the many-body problems onto a Hilbert subspace spanned by a limited set of Krylov bases that can be handled on the classical computer. Then, one solves the Hamiltonian eigenvalue problem in the Krylov subspace for the eigenenergies of the low-lying states on the classical computer. We present more details of the CP-QKSD method in Appendix A.

TABLE II. Information of the many-boson Hamiltonian $H_{K=4}$ for the circuit design of the Hamiltonian input scheme. The first, second, and third columns list the index j , the circuit modules of the combinations of the squeezed boson operators, and the coefficient of each monomial, respectively.

index j	circuit modules	B'_j [MeV ²]	index j	circuit modules	B'_j [MeV ²]
0	$(+-)_1$	4	7	$(-)_1(++)_2(-)_3$	4.24866
1	$(+-)_2$	1	8	$(+)_1(--)_2(+)_3$	4.24866
2	$(+-)_3$	1/3	9	$(+ + --)_2$	1.83972
3	$(+-)_4$	1/4	10	$(- - -)_1(+)_3$	5.66488
4	$(+ + --)_1$	29.4356	11	$(--)_1(-)_2(+)_4$	7.35889
5	$(+-)_1(+)_2$	29.4356	12	$(+ + +)_1(-)_3$	5.66488
6	$(+-)_1(+)_3$	9.81186	13	$(++)_1(+)_2(-)_4$	7.35889

We retain a limited model problem with $K = 4$ in our numerical demonstration. We elect $m^2 = 1$ MeV² and $\lambda/m^2 = 92.4746$ for the $(\phi^4)_2$ theory, where the reasons for this parameter setup will be clear in the following text. The LF Hamiltonian for the $(\phi^4)_2$ theory in terms of the squeezed boson operators [Eq. (15)] reads

$$\begin{aligned}
H_{K=4} = & B'_0 b_1^\dagger b_1 + B'_1 b_2^\dagger b_2 + B'_2 b_3^\dagger b_3 + B'_3 b_4^\dagger b_4 + B'_4 b_1^\dagger b_1^\dagger b_1 b_1 + B'_5 b_1^\dagger b_1 b_2^\dagger b_2 \\
& + B'_6 b_1^\dagger b_1 b_3^\dagger b_3 + B'_7 b_1 b_2^\dagger b_2^\dagger b_3 + B'_8 b_1^\dagger b_2 b_2 b_3^\dagger + B'_9 b_2^\dagger b_2^\dagger b_2 b_2 + B'_{10} b_1 b_1 b_1 b_3^\dagger \\
& + B'_{11} b_1 b_1 b_2 b_4^\dagger + B'_{12} b_1^\dagger b_1^\dagger b_1^\dagger b_3 + B'_{13} b_1^\dagger b_1^\dagger b_2^\dagger b_4.
\end{aligned} \tag{41}$$

For clarity, we present the indices of the monomials of $H_{K=4}$ in Table II, where we also list the coefficient and the corresponding circuit modules (Table I) for each monomial. With this, we design the quantum walk states and present the corresponding input scheme of the second-quantized many-boson Hamiltonian according to Eq. (39), where we take $\Xi = B'_4 = 29.4356$ MeV².

We note that there are five many-boson bases for our model problem with $K = 4$. These bases can be sorted into two sectors according to the evenness and oddness of the particle number as $\mathcal{B}_{\text{even}} = \{|3^1, 1^1\rangle, |2^2\rangle, |1^4\rangle\}$ and $\mathcal{B}_{\text{odd}} = \{|4^1\rangle, |2^1, 1^2\rangle\}$. The many-boson Hamiltonian matrix in the basis $\mathcal{B}_{K=4} = \mathcal{B}_{\text{even}} \oplus \mathcal{B}_{\text{odd}}$ is

$$H_{K=4} = \begin{pmatrix} 3.78630 & 1.50213 & 3.46902 & & & \\ 1.50213 & 1.91986 & 0 & & & \\ 3.46902 & 0 & 26.0767 & & & \\ & & & 0.25 & 1.83972 & \\ & & & 1.83972 & 13.5383 & \end{pmatrix}, \tag{42}$$

in units of MeV². We find that the Hamiltonian matrix is block diagonal. This is due to the fact that the LF Hamiltonian [Eq. (3)] preserves the symmetry of oddness and evenness. By straightforward matrix diagonalization, we obtain the eigenvalues of $H_{K=4}$ to be $E_0 = 1.61752 \times 10^{-7}$ MeV², $E_1 = 0.958969$ MeV², $E_2 = 4.21772$ MeV², $E_3 = 13.7883$ MeV², $E_4 = 26.6062$ MeV², where E_0 and E_3 are the eigenvalues for the odd-particle-number sector (lower-right submatrix), while the others are the eigenvalues for the even-particle-number sector (upper-left submatrix).

We adopt the CP-QKSD method [76] in the eigenvalue calculations of $H_{K=4}$ with the strategy shown in Ref. [50]. We note that our Hamiltonian input scheme respects the symmetry (the evenness and oddness) of the many-boson system. Therefore, we can generate the Krylov bases with specific symmetry by preparing the many-boson pivot state $|\psi_0\rangle$ to be of the desired symmetry (this preparation is straightforward in the framework of second quantization) on the quantum computer. Based on the symmetry-adapted Krylov basis set, we evaluate the Hamiltonian and the overlap matrix elements implementing the noiseless Statevector simulator of the IBM Qiskit package [72]. These matrix elements are used to construct the generalized eigenvalue problems on the classical computer to solve for the ground-state eigenvalues in the symmetry-adapted Hilbert subspaces.

Within the Hilbert subspace of odd particle numbers, we obtain the ground-state eigenenergy to be 1.61752×10^{-7} MeV². On the other hand, the ground state eigenvalue is 0.958969 MeV² when we work in the subspace of even particle numbers. These eigenenergies agree with those from the classical calculations. The small ground-state eigenvalue in the odd-particle-number sector implies a vanishing mass gap [Eq. (9)]. This indicates that the coupling constant $\lambda/m^2 = 92.4746$ is close to the critical coupling for the $(\phi^4)_2$ theory at $K = 4$.

For the $(\phi^4)_2$ theory in the DLCQ framework, we expect that our input scheme can face numerical challenges in the setup when we do not truncate the number of particles and when the strong coupling constant $\lambda/m^2 \gg 1$ is retained in the many-body interaction term. However, one does not expect these challenging cases in many field theory problems of higher spatial dimensions, such as the $(d+1)$ -dimensional ϕ^4 (with $d \geq 2$) theory, and other realistic field theory problems such as quantum electrodynamics, quantum chromodynamics, or chiral effective field theories. In such field theory problems, the coupling strengths are small, and it is reasonable to restrict the number of constituent particles in a physical system utilizing the schemes of the Fock-sector expansion and truncation within the LF Hamiltonian formalism. With such considerations, we expect that our input scheme can be adopted to treat these theories [21, 23, 24] in a straightforward manner.

V. SUMMARY AND OUTLOOK

In this work, we propose a novel input scheme for second-quantized many-boson Hamiltonians in quantum computing. For clarity, we present the input scheme utilizing the simple two-dimensional ϕ^4 theory within the Hamiltonian formalism obtained by the discretized light-cone discretization approach.

In our input scheme, we employ a set of registers to encode the many-boson states, where each register encodes the occupation of a specific boson mode in binaries. We also squeeze the boson operators of each mode with the maximal occupation number of the mode. For all the monomials in the light-front (LF) many-boson Hamiltonian, we find a limited set of unique combinations of the squeezed-boson operators, and we rewrite the Hamiltonian in terms of these unique combinations. In this work, we present explicit design for the circuit modules (or circuit representation) for these combinations. Based on these modules, we prepare the quantum walk states according to the many-boson Hamiltonian. With these walk states, we block encode the many-boson Hamiltonian.

For demonstration purposes, we present the spectral calculations of the LF Hamiltonian of the two-dimensional ϕ^4 theory in a restricted model space based on our Hamiltonian input scheme and implementing the hybrid algorithm of the quantum Krylov subspace diagonalization [76]. We perform our quantum computations utilizing the noiseless Statevector simulator of the IBM Qiskit package [72], of which the results are post-processed on the classical computer for the eigenenergies of the low-lying states. Our results of the hybrid quantum-classical calculations agree with those from pure classical calculations.

Our input scheme can be applied to treat other field theory problems, e.g., quantum electrodynamics, quantum chromodynamics, or chiral field theories [e.g., Ref. [38]]. Combined with the input scheme for the second-quantized many-fermion Hamiltonians [49, 50], our input scheme for the second-quantized many-boson Hamiltonians opens up a novel and systematic path for solving the structure and dynamics of quantum field theory on future fault-tolerant quantum computers.

ACKNOWLEDGEMENTS

We acknowledge fruitful discussions with Peter Love, Chao Yang, Pieter Maris, Michael Kreshchuk, and Shreeram Jawadekar. This work was supported by US DOE Grant DE-SC0023707 under the Office of Nuclear Physics Quantum Horizons program for the “**Nu**Nuclei and **Had**rons with **Q**uantum computers (**NuHaQ**)” project.

Appendix A: CP-QKSD method

We present the details of the CP-QKSD algorithm [76] applied in our numerical demonstration. The CP-QKSD algorithm computes the eigenvalues of the low-lying states of the Hamiltonian based on the block-encoded Hamiltonian in quantum computing. Interested readers are also referred to Ref. [77] and references therein for a general review of various other quantum-subspace methods for structure calculations.

As for this work, our input scheme is designed to block encode the second-quantized LF Hamiltonian as [Eq. (39)]

$$\langle \langle \mathcal{G} |_s \otimes \langle 0 |_a \rangle \mathcal{T}_2^\dagger \mathcal{T}_1 (|\mathcal{F}\rangle_s \otimes |0\rangle_a) = \frac{1}{\mathcal{D}\Xi} \langle \mathcal{G} | H | \mathcal{F} \rangle.$$

With this Hamiltonian input model, we can construct the input scheme of the Chebyshev polynomials of the first kind [78] as functions of $H' = H/(\mathcal{D}\Xi)$:

$$\langle \psi_0 | T_{2k+1}(H') | \psi_0 \rangle = \langle \langle \psi_0 |_s \otimes \langle 0 |_a \rangle [U_H \Pi (U_H^\dagger \Pi U_H \Pi)^k] (|\psi_0\rangle_s \otimes |0\rangle_a), \quad (\text{A1})$$

$$\langle \psi_0 | T_{2k}(H') | \psi_0 \rangle = \langle \langle \psi_0 |_s \otimes \langle 0 |_a \rangle (U_H^\dagger \Pi U_H \Pi)^k (|\psi_0\rangle_s \otimes |0\rangle_a), \quad (\text{A2})$$

with $k = 0, 1, 2, \dots$. Here we define $U_H \equiv \mathcal{T}_2^\dagger \mathcal{T}_1$. The reflection operator $\Pi \equiv (2|0\rangle_a \langle 0|_a - \mathbb{I}_a) \otimes \mathbb{I}_s$ produces the reflection around $|0\rangle_a$ in the auxiliary space. The quantum circuit to input $T_j(H')$ is achieved via **alternating** applications of $U_H \Pi$ and $U_H^\dagger \Pi$ [50, 79].

We can construct the Krylov basis as [76]

$$\{ |\psi_i\rangle = T_i(H') | \psi_0 \rangle \mid i = 0, 1, 2, \dots, \mathcal{K} - 1 \}, \quad (\text{A3})$$

where $|\psi_0\rangle$ denotes the pivot many-boson state.

In the Krylov basis, the matrix element of H' is

$$H'_{ij} = \langle \psi_i | H' | \psi_j \rangle = \langle \psi_0 | T_i(H') H' T_j(H') | \psi_0 \rangle, \quad (\text{A4})$$

while the element of the overlap matrix S is

$$S_{ij} = \langle \psi_i | \psi_j \rangle = \langle \psi_0 | T_i(H') T_j(H') | \psi_0 \rangle. \quad (\text{A5})$$

Utilizing the identities of the Chebyshev polynomials [78]

$$T_0(x) = 1, \quad T_1(x) = x, \quad T_i(x) T_j(x) = [T_{i+j}(x) + T_{|i-j|}(x)]/2, \quad (\text{A6})$$

one can express H'_{ij} and S_{ij} in terms of the expectation $\langle T_k(H') \rangle_0 \equiv \langle \psi_0 | T_k(H') | \psi_0 \rangle$.

The expectation values $\{\langle T_k(H') \rangle_0\}$ are, in general, challenging to calculate on classical computers for quantum many-body systems, while they are expected to be evaluated with efficiency on quantum computers [3]. We can then compute these expectation values on quantum computers and input them to the classical computer to compute $\{H'_{ij}\}$ and $\{S_{ij}\}$, based on which we construct the generalized eigenvalue problem

$$H' |\varphi\rangle = \mathcal{E} S |\varphi\rangle, \quad (\text{A7})$$

where \mathcal{E} denotes the eigenvalue of the eigenstate $|\varphi\rangle$.

A general bound of \mathcal{K} [Eq. (A3)] to compute the ground state energy with the error ϵ is [76]

$$\mathcal{K} = \Theta[(\log |\kappa_0|^{-1} + \log \epsilon^{-1}) \cdot \min(\epsilon^{-1}, \delta^{-1})], \quad (\text{A8})$$

where κ_0 denotes the overlap between the pivot $|\psi_0\rangle$ and the ground state. δ is the spectral gap between the ground and first-excited state. One notes also that the overlap matrix is, in general, ill conditioned. In practical calculations, one can adopt the canonical orthogonalization [80] for approximating the lowest eigenvalue of H' [81].

As noted in Ref. [50], our Hamiltonian input scheme, which operates in the framework of second-quantization, offers a natural advantage in implementing the CP-QKSD algorithm. Indeed, the occupation representation makes it straightforward and convenient to prepare a pivot $|\psi_0\rangle$ to be of specific symmetries of the Hamiltonian. Therefore, we can naturally generate a Krylov basis set $\{|\psi_i\rangle\}$ [Eq. (A3)] with elected symmetries. In this way, we are able to work within a particular symmetry-adopted Hilbert subspace and solve for the eigenenergy of corresponding ground state with the elected symmetries, where the unwanted states that do not respect the elected symmetries are naturally excluded.

[1] M. Peskin, *An Introduction To Quantum Field Theory* (CRC Press, 2018).

- [2] J. Preskill, Quantum Computing in the NISQ era and beyond, *Quantum* **2**, 79 (2018).
- [3] R. P. Feynman, Simulating physics with computers, *International Journal of Theoretical Physics* **21** (1982).
- [4] S. P. Jordan, K. S. M. Lee, and J. Preskill, Quantum algorithms for quantum field theories, *Science* **336**, 1130 (2012).
- [5] N. Klco, E. F. Dumitrescu, A. J. McCaskey, T. D. Morris, R. C. Pooser, M. Sanz, E. Solano, P. Lougovski, and M. J. Savage, Quantum-classical computation of schwinger model dynamics using quantum computers, *Phys. Rev. A* **98**, 032331 (2018).
- [6] N. Klco and M. J. Savage, Digitization of scalar fields for quantum computing, *Phys. Rev. A* **99**, 052335 (2019).
- [7] N. Klco, M. J. Savage, and J. R. Stryker, $Su(2)$ non-abelian gauge field theory in one dimension on digital quantum computers, *Phys. Rev. D* **101**, 074512 (2020).
- [8] M. Rhodes, M. Kreshchuk, and S. Pathak, Exponential improvements in the simulation of lattice gauge theories using near-optimal techniques, (2024), [arXiv:2405.10416](https://arxiv.org/abs/2405.10416) [quant-ph].
- [9] C. W. Bauer, Z. Davoudi, A. B. Balantekin, T. Bhattacharya, M. Carena, W. A. de Jong, P. Draper, A. El-Khadra, N. Gemelke, M. Hanada, D. Kharzeev, H. Lamm, Y.-Y. Li, J. Liu, M. Lukin, Y. Meurice, C. Monroe, B. Nachman, G. Pagano, J. Preskill, E. Rinaldi, A. Roggero, D. I. Santiago, M. J. Savage, I. Siddiqi, G. Siopsis, D. V. Zanten, N. Wiebe, Y. Yamauchi, K. Yeter-Aydeniz, and S. Zorzetti, Quantum simulation for high energy physics (2022), [arXiv:2204.03381](https://arxiv.org/abs/2204.03381) [quant-ph].
- [10] C. W. Bauer, Z. Davoudi, N. Klco, and M. J. Savage, Quantum simulation of fundamental particles and forces, *Nature Rev. Phys.* **5**, 420 (2023), [arXiv:2404.06298](https://arxiv.org/abs/2404.06298) [hep-ph].
- [11] B. Müller and X. Yao, Simple Hamiltonian for quantum simulation of strongly coupled (2+1)D $SU(2)$ lattice gauge theory on a honeycomb lattice, *Phys. Rev. D* **108**, 094505 (2023), [arXiv:2307.00045](https://arxiv.org/abs/2307.00045) [quant-ph].
- [12] C. W. Bauer and D. M. Grabowska, Efficient representation for simulating $U(1)$ gauge theories on digital quantum computers at all values of the coupling, *Phys. Rev. D* **107**, L031503 (2023), [arXiv:2111.08015](https://arxiv.org/abs/2111.08015) [hep-ph].
- [13] A. N. Ciavarella and C. W. Bauer, Quantum Simulation of $SU(3)$ Lattice Yang Mills Theory at Leading Order in Large N , (2024), [arXiv:2402.10265](https://arxiv.org/abs/2402.10265) [hep-ph].
- [14] I. D'Andrea, C. W. Bauer, D. M. Grabowska, and M. Freytsis, New basis for Hamiltonian $SU(2)$ simulations, *Phys. Rev. D* **109**, 074501 (2024), [arXiv:2307.11829](https://arxiv.org/abs/2307.11829) [hep-ph].
- [15] S. Hariprakash, N. S. Modi, M. Kreshchuk, C. F. Kane, and C. W. Bauer, Strategies for simulating time evolution of Hamiltonian lattice field theories, (2023), [arXiv:2312.11637](https://arxiv.org/abs/2312.11637) [quant-ph].
- [16] Z. Davoudi, C.-C. Hsieh, and S. V. Kadam, Scattering wave packets of hadrons in gauge theories: Preparation on a quantum computer, (2024), [arXiv:2402.00840](https://arxiv.org/abs/2402.00840) [quant-ph].
- [17] J. D. Watson, J. Bringewatt, A. F. Shaw, A. M. Childs, A. V. Gorshkov, and Z. Davoudi, Quantum Algorithms for Simulating Nuclear Effective Field Theories, (2023), [arXiv:2312.05344](https://arxiv.org/abs/2312.05344) [quant-ph].
- [18] Z. Davoudi, A. F. Shaw, and J. R. Stryker, General quantum algorithms for Hamiltonian simulation with applications to a non-Abelian lattice gauge theory, *Quantum* **7**, 1213 (2023), [arXiv:2212.14030](https://arxiv.org/abs/2212.14030) [hep-lat].
- [19] N. Mueller, J. A. Carolan, A. Connelly, Z. Davoudi, E. F. Dumitrescu, and K. Yeter-Aydeniz, Quantum Computation of Dynamical Quantum Phase Transitions and Entanglement Tomography in a Lattice Gauge Theory, *PRX Quantum* **4**, 030323 (2023), [arXiv:2210.03089](https://arxiv.org/abs/2210.03089) [quant-ph].
- [20] M. Rhodes L., M. Kreshchuk, and A. J. Landahl, Fault-tolerant quantum simulation algorithms for computing particle masses and other relativistic bound-state properties in quantum chromodynamics (2024), manuscript in preparation.
- [21] P. A. M. Dirac, Forms of relativistic dynamics, *Rev. Mod. Phys.* **21**, 392 (1949).
- [22] P. A. M. Dirac, Generalized hamiltonian dynamics, *Canadian Journal of Mathematics* **2**, 129–148 (1950).
- [23] S. J. Brodsky, H.-C. Pauli, and S. S. Pinsky, Quantum chromodynamics and other field theories on the light cone, *Physics Reports* **301**, 299 (1998).
- [24] J. P. Vary, H. Honkanen, J. Li, P. Maris, S. J. Brodsky, A. Harindranath, G. F. de Teramond, P. Sternberg, E. G. Ng, and C. Yang, Hamiltonian light-front field theory in a basis function approach, *Phys. Rev. C* **81**, 035205 (2010), [arXiv:0905.1411](https://arxiv.org/abs/0905.1411) [nucl-th].
- [25] M. Li, Y. Li, P. Maris, and J. P. Vary, Radiative transitions between 0^{++} and 1^{--} heavy quarkonia on the light front, *Phys. Rev. D* **98**, 034024 (2018), [arXiv:1803.11519](https://arxiv.org/abs/1803.11519) [hep-ph].
- [26] M. Li, X. Zhao, P. Maris, G. Chen, Y. Li, K. Tuchin, and J. P. Vary, Ultrarelativistic quark-nucleus scattering in a light-front Hamiltonian approach, *Phys. Rev. D* **101**, 076016 (2020), [arXiv:2002.09757](https://arxiv.org/abs/2002.09757) [nucl-th].
- [27] M. Li, T. Lappi, and X. Zhao, Scattering and gluon emission in a color field: A light-front Hamiltonian approach, *Phys. Rev. D* **104**, 056014 (2021), [arXiv:2107.02225](https://arxiv.org/abs/2107.02225) [hep-ph].
- [28] X. Zhao, A. Ilderton, P. Maris, and J. P. Vary, Scattering in Time-Dependent Basis Light-Front Quantization, *Phys. Rev. D* **88**, 065014 (2013), [arXiv:1303.3273](https://arxiv.org/abs/1303.3273) [nucl-th].
- [29] X. Zhao, A. Ilderton, P. Maris, and J. P. Vary, Non-perturbative quantum time evolution on the light-front, *Phys. Lett. B* **726**, 856 (2013), [arXiv:1309.5338](https://arxiv.org/abs/1309.5338) [nucl-th].
- [30] S. Xu, C. Mondal, J. Lan, X. Zhao, Y. Li, and J. P. Vary (BLFQ), Nucleon structure from basis light-front quantization, *Phys. Rev. D* **104**, 094036 (2021), [arXiv:2108.03909](https://arxiv.org/abs/2108.03909) [hep-ph].
- [31] C. Mondal, S. Xu, J. Lan, X. Zhao, Y. Li, D. Chakrabarti, and J. P. Vary, Proton structure from a light-front Hamiltonian, *Phys. Rev. D* **102**, 016008 (2020), [arXiv:1911.10913](https://arxiv.org/abs/1911.10913) [hep-ph].
- [32] J. Lan, C. Mondal, S. Jia, X. Zhao, and J. P. Vary, Pion and kaon parton distribution functions from basis light front quantization and QCD evolution, *Phys. Rev. D* **101**, 034024 (2020), [arXiv:1907.01509](https://arxiv.org/abs/1907.01509) [nucl-th].
- [33] P. Wiecki, Y. Li, X. Zhao, P. Maris, and J. P. Vary, Basis Light-Front Quantization Approach to Positronium, *Phys. Rev. D* **91**, 105009 (2015), [arXiv:1404.6234](https://arxiv.org/abs/1404.6234) [nucl-th].

- [34] X. Zhao, H. Honkanen, P. Maris, J. P. Vary, and S. J. Brodsky, Electron $g-2$ in Light-Front Quantization, *Phys. Lett. B* **737**, 65 (2014), [arXiv:1402.4195 \[nucl-th\]](#).
- [35] Y. Li, P. Maris, and J. P. Vary, Quarkonium as a relativistic bound state on the light front, *Phys. Rev. D* **96**, 016022 (2017), [arXiv:1704.06968 \[hep-ph\]](#).
- [36] Y. Li, P. Maris, X. Zhao, and J. P. Vary, Heavy Quarkonium in a Holographic Basis, *Phys. Lett. B* **758**, 118 (2016), [arXiv:1509.07212 \[hep-ph\]](#).
- [37] W. Qian, S. Jia, Y. Li, and J. P. Vary, Light mesons within the basis light-front quantization framework, *Phys. Rev. C* **102**, 055207 (2020), [arXiv:2005.13806 \[nucl-th\]](#).
- [38] W. Du, Y. Li, X. Zhao, G. A. Miller, and J. P. Vary, Basis Light-Front Quantization for a Chiral Nucleon-Pion Lagrangian, *Phys. Rev. C* **101**, 035202 (2020), [arXiv:1911.10762 \[nucl-th\]](#).
- [39] S. Jia and J. P. Vary, Basis light front quantization for the charged light mesons with color singlet Nambu–Jona-Lasinio interactions, *Phys. Rev. C* **99**, 035206 (2019), [arXiv:1811.08512 \[nucl-th\]](#).
- [40] H. Honkanen, P. Maris, J. P. Vary, and S. J. Brodsky, Electron in a transverse harmonic cavity, *Phys. Rev. Lett.* **106**, 061603 (2011), [arXiv:1008.0068 \[hep-ph\]](#).
- [41] M. Kreshchuk, S. Jia, W. M. Kirby, G. Goldstein, J. P. Vary, and P. J. Love, Simulating Hadronic Physics on NISQ devices using Basis Light-Front Quantization, *Phys. Rev. A* **103**, 062601 (2021), [arXiv:2011.13443 \[quant-ph\]](#).
- [42] M. Kreshchuk, W. M. Kirby, G. Goldstein, H. Beauchemin, and P. J. Love, Quantum simulation of quantum field theory in the light-front formulation, *Phys. Rev. A* **105**, 032418 (2022), [arXiv:2002.04016 \[quant-ph\]](#).
- [43] M. Kreshchuk, S. Jia, W. M. Kirby, G. Goldstein, J. P. Vary, and P. J. Love, Light-Front Field Theory on Current Quantum Computers, *Entropy* **23**, 597 (2021), [arXiv:2009.07885 \[quant-ph\]](#).
- [44] W. Qian, R. Basili, S. Pal, G. Luecke, and J. P. Vary, Solving hadron structures using the basis light-front quantization approach on quantum computers, *Phys. Rev. Res.* **4**, 043193 (2022), [arXiv:2112.01927 \[quant-ph\]](#).
- [45] J. a. Barata, X. Du, M. Li, W. Qian, and C. A. Salgado, Quantum simulation of in-medium QCD jets: Momentum broadening, gluon production, and entropy growth, *Phys. Rev. D* **108**, 056023 (2023), [arXiv:2307.01792 \[hep-ph\]](#).
- [46] J. a. Barata, X. Du, M. Li, W. Qian, and C. A. Salgado, Medium induced jet broadening in a quantum computer, *Phys. Rev. D* **106**, 074013 (2022), [arXiv:2208.06750 \[hep-ph\]](#).
- [47] X. Yao, Quantum Simulation of Light-Front QCD for Jet Quenching in Nuclear Environments, (2022), [arXiv:2205.07902 \[hep-ph\]](#).
- [48] S. Wu, W. Du, X. Zhao, and J. P. Vary, Ultra-relativistic quark-nucleus scattering on quantum computers, (2024), [arXiv:2404.00819 \[quant-ph\]](#).
- [49] W. Du and J. P. Vary, Multinucleon structure and dynamics via quantum computing, *Phys. Rev. A* **108**, 052614 (2023), [arXiv:2304.04838 \[nucl-th\]](#).
- [50] W. Du and J. P. Vary, Hamiltonian input model and spectroscopy on quantum computers, (2024), [arXiv:2402.08969 \[quant-ph\]](#).
- [51] E. Merzbacher, *Quantum Mechanics* (Wiley, 1998).
- [52] A. M. Childs, On the relationship between continuous-and discrete-time quantum walk, *Communications in Mathematical Physics* **294**, 581 (2010).
- [53] D. W. Berry and A. M. Childs, Black-box hamiltonian simulation and unitary implementation, *Quantum Information and Computation* **12**, 29 (2012).
- [54] A. M. Childs and N. Wiebe, Hamiltonian simulation using linear combinations of unitary operations, *Quantum Inf. Comput.* **12**, 901 (2012).
- [55] R. Babbush, D. Berry, I. Kivlichan, A. Wei, P. Love, and A. Aspuru-Guzik, Exponentially more precise quantum simulation of fermions in second quantization, *New Journal of Physics* **18**, 033032 (2016).
- [56] W. M. Kirby, S. Hadi, M. Kreshchuk, and P. J. Love, Quantum simulation of second-quantized hamiltonians in compact encoding, *Phys. Rev. A* **104**, 042607 (2021).
- [57] A. M. Childs, Universal computation by quantum walk, *Phys. Rev. Lett.* **102**, 180501 (2009).
- [58] G. H. Low and I. L. Chuang, Optimal hamiltonian simulation by quantum signal processing, *Phys. Rev. Lett.* **118**, 010501 (2017).
- [59] A. Gilyén, Y. Su, G. H. Low, and N. Wiebe, Quantum singular value transformation and beyond: exponential improvements for quantum matrix arithmetics, in *Proceedings of the 51st Annual ACM SIGACT Symposium on Theory of Computing* (2019) pp. 193–204.
- [60] J. M. Martyn, Z. M. Rossi, A. K. Tan, and I. L. Chuang, Grand unification of quantum algorithms, *PRX Quantum* **2**, 040203 (2021).
- [61] Y. Dong, L. Lin, and Y. Tong, Ground-state preparation and energy estimation on early fault-tolerant quantum computers via quantum eigenvalue transformation of unitary matrices, *PRX Quantum* **3**, 040305 (2022).
- [62] A. Harindranath and J. P. Vary, Solving two dimensional ϕ^4 theory by discretized light front quantization, *Phys. Rev. D* **36**, 1141 (1987).
- [63] J. P. Vary, M. Huang, S. Jawadekar, M. Sharaf, A. Harindranath, and D. Chakrabarti, Critical coupling for two-dimensional ϕ^4 theory in discretized light-cone quantization, *Phys. Rev. D* **105**, 016020 (2022).
- [64] H. C. Pauli and S. J. Brodsky, Discretized Light Cone Quantization: Solution to a Field Theory in One Space One Time Dimensions, *Phys. Rev. D* **32**, 2001 (1985).
- [65] H. C. Pauli and S. J. Brodsky, Solving Field Theory in One Space One Time Dimension, *Phys. Rev. D* **32**, 1993 (1985).
- [66] T. Eller, H. C. Pauli, and S. J. Brodsky, Discretized Light Cone Quantization: The Massless and the Massive Schwinger Model, *Phys. Rev. D* **35**, 1493 (1987).

- [67] S.-J. Chang, Existence of a second-order phase transition in a two-dimensional ϕ^4 field theory, *Phys. Rev. D* **13**, 2778 (1976).
- [68] S. Coleman, Quantum sine-gordon equation as the massive thirring model, *Phys. Rev. D* **11**, 2088 (1975).
- [69] M. Burkardt, S. S. Chabysheva, and J. R. Hiller, Two-dimensional light-front ϕ^4 theory in a symmetric polynomial basis, *Phys. Rev. D* **94**, 065006 (2016).
- [70] N. Anand, V. X. Genest, E. Katz, Z. U. Khandker, and M. T. Walters, RG flow from ϕ^4 theory to the 2D Ising model, *JHEP* **08**, 056, [arXiv:1704.04500](https://arxiv.org/abs/1704.04500) [hep-th].
- [71] S. S. Chabysheva and J. R. Hiller, Tadpoles and vacuum bubbles in light-front quantization, *Phys. Rev. D* **105**, 116006 (2022), [arXiv:2201.00123](https://arxiv.org/abs/2201.00123) [hep-th].
- [72] Qiskit contributors, *Qiskit: An open-source framework for quantum computing* (2023).
- [73] E. Rieffel and W. Polak, *Quantum Computing: A Gentle Introduction*, Scientific and Engineering Computation (MIT Press, 2011).
- [74] A. JavadiAbhari, S. Patil, D. Kudrow, J. Heckey, A. Lvov, F. T. Chong, and M. Martonosi, Scaffcc: Scalable compilation and analysis of quantum programs, *Parallel Computing* **45**, 2 (2015).
- [75] A. JavadiAbhari, S. Patil, D. Kudrow, J. Heckey, A. Lvov, F. T. Chong, and M. Martonosi, Scaffcc: a framework for compilation and analysis of quantum computing programs, in *Proceedings of the 11th ACM Conference on Computing Frontiers*, CF '14 (Association for Computing Machinery, New York, NY, USA, 2014).
- [76] W. Kirby, M. Motta, and A. Mezzacapo, Exact and efficient lanczos method on a quantum computer, *Quantum* **7**, 1018 (2023).
- [77] M. Motta, W. Kirby, I. Liepuoniute, K. J. Sung, J. Cohn, A. Mezzacapo, K. Klymko, N. Nguyen, N. Yoshioka, and J. E. Rice, Subspace methods for electronic structure simulations on quantum computers (2023), [arXiv:2312.00178](https://arxiv.org/abs/2312.00178) [quant-ph].
- [78] G. Arfken, G. Arfken, H. Weber, and F. Harris, *Mathematical Methods for Physicists: A Comprehensive Guide* (Elsevier Science, 2013).
- [79] L. Lin, Lecture notes on quantum algorithms for scientific computation (2022), [arXiv:2201.08309](https://arxiv.org/abs/2201.08309) [quant-ph].
- [80] P.-O. Löwdin, On the nonorthogonality problem, *Advances in Quantum Chemistry*, **5**, 185 (1970).
- [81] E. N. Epperly, L. Lin, and Y. Nakatsukasa, A theory of quantum subspace diagonalization, *SIAM Journal on Matrix Analysis and Applications* **43**, 1263 (2022), <https://doi.org/10.1137/21M145954X>.